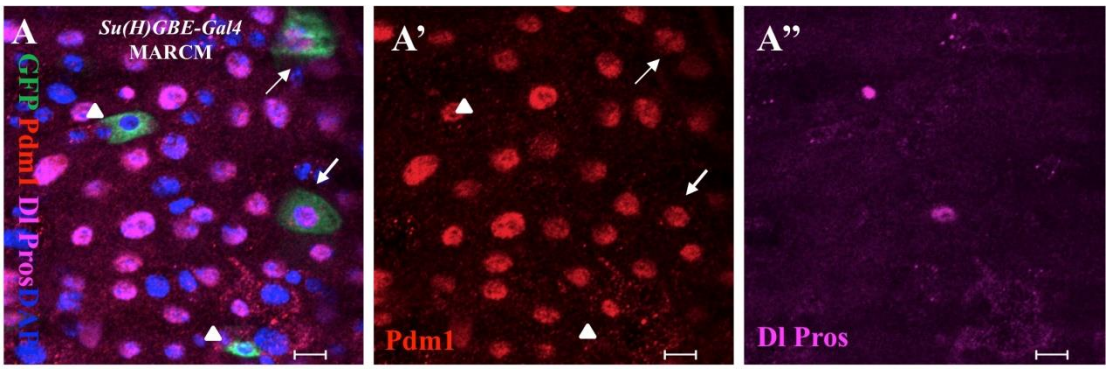

Fig. S1. ECs, but not EEs, develop from Su(H)GBE$^+$ EBs

(A-A'') MARCM clones using *Su(H)GBE-Gal4* instead of *Tub-Gal4*. Some Pdm1$^+$ ECs (arrow) inherited weak GFP from Su(H)GBE$^+$ EBs (arrowhead), but none of the EEs inherited GFP from Su(H)GBE$^+$ EBs. The genotype is *hs-flp, tub-Gal80, FRT19A/FRT19A, sn3, w1118; Su(H)GBE-Gal4, UAS-mCD8-GFP*.

The adult fly posterior midguts were stained with anti-GFP (green), anti-Pdm1 (red), anti-Dl (cytoplasmic, purple), anti-Pros (nuclear, purple), and DAPI (blue). Scale bars, 10 μm.

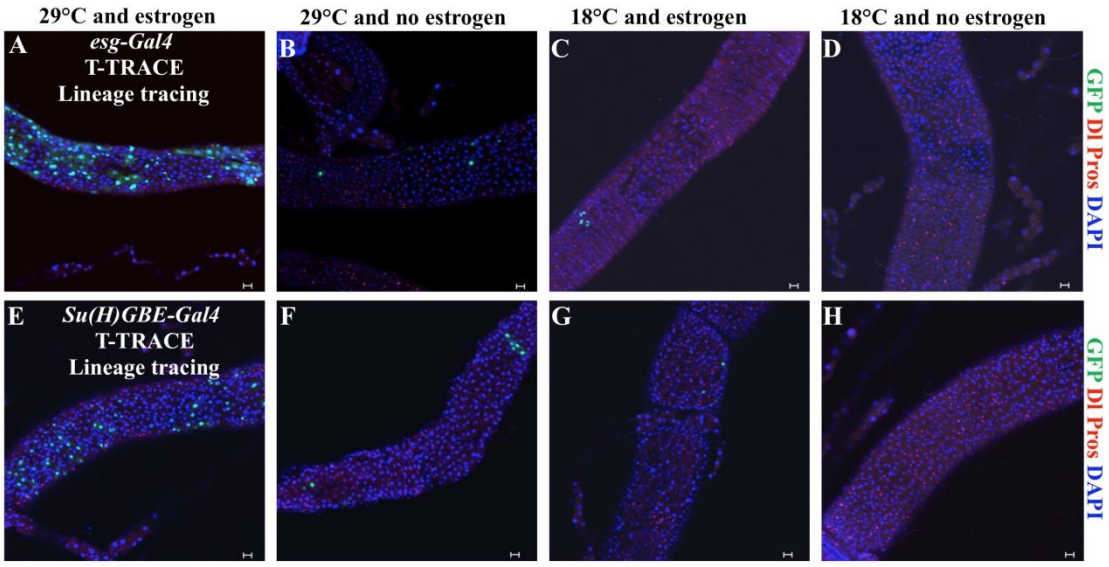

I

Percentage of guts that have at least one GFP-positive cell

Genotype/Culture condition	29°C and estrogen	29°C and no estrogen	18°C and estrogen	18°C and no estrogen
esg-Gal4/T-TRACE	100% (n=29)	35.4% (n=48)	17.3% (n=52)	1.8% (n=57)
Su(H)GBE-Gal4/T-TRACE	100% (n=38)	39.0% (n=41)	18.8% (n=32)	0% (n=45)

Fig. S2. The T-TRACE analysis system.

(A-D) Fluorescence images showing T-TRACE analysis of the *esg-Gal4* line at 29°C on food with estrogen (A), at 29°C on food without estrogen (B), at 18°C on food with estrogen (C), and at 18°C on food without estrogen (D).

(E-H) Fluorescence images showing T-TRACE analysis of the *Su(H)GBE-Gal4* line at 29°C on food with estrogen (E), at 29°C on food without estrogen (F), at 18°C on food with estrogen (G), and at 18°C on food without estrogen (H). The adult fly posterior midguts were stained with anti-GFP (green), anti-Dl (cytoplasmic, red), anti-Pros (nuclear, red), and DAPI (blue). Scale bars, 20 μm.

(I) The quantitative percentage of guts containing at least one GFP-positive cell in each of the above conditions.

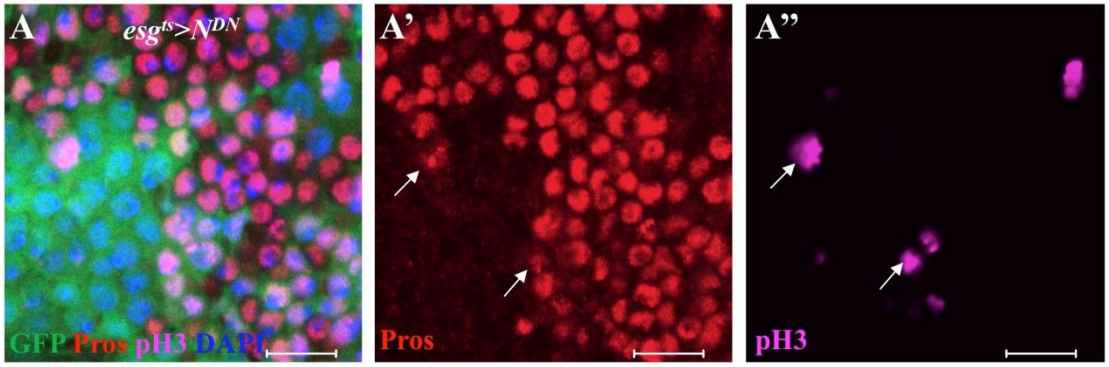

Fig. S3. Some of the dividing ISC-like cells express Pros.

(A-A'') Pros^{+} cells in the N^{DN} midgut are undergoing cell division in the N^{DN} midgut (arrow).

The adult fly posterior midguts were stained anti-GFP (green), anti-Pros (red), anti-pH3 (purple), and DAPI (blue). Scale bars, 10 μm.

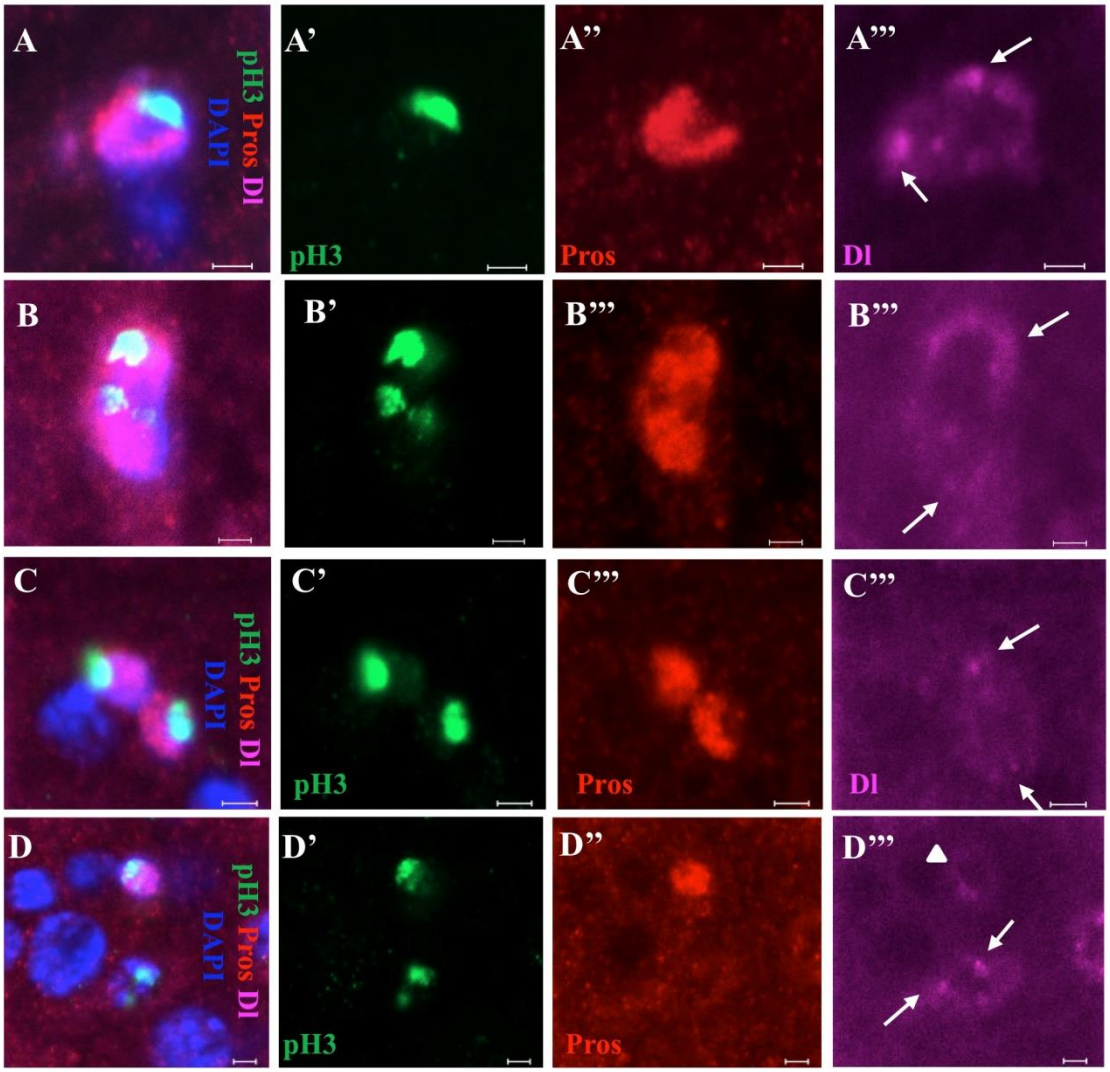

Fig. S4. EEs are generated from ISCs through pre-EEs.

(A-A''') A dividing Dl^+ ISC at pre-prophase expresses EE marker Pros.

(B-B''') A dividing ISC at early telophase generates two Dl^+ $Pros^+$ pre-EEs by symmetric division.

(C-C''') A dividing ISC at late telophase generates two Dl^+ $Pros^+$ pre-EEs by symmetric division.

(D-D''') A dividing ISC at late telophase generates one Dl^+ $Pros^+$ pre-EE and one Dl^+ $Pros^-$ ISC by asymmetric division.

The adult fly posterior midguts were stained with anti-pH3 (green), anti-Pros (red), anti-Dl (purple), and DAPI (blue). Scale bars, 2 μm.

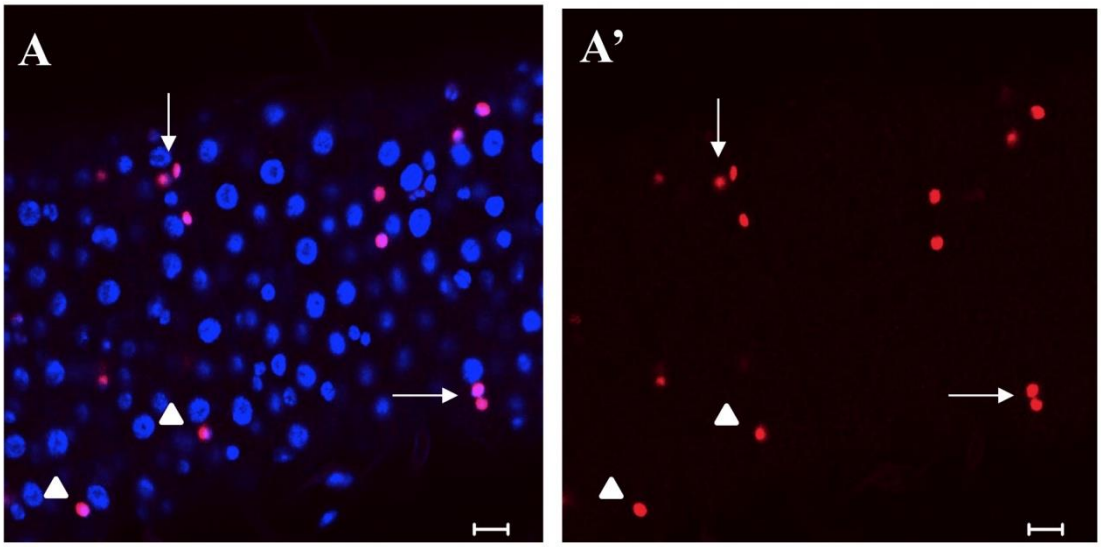

Fig. S5. Single EEs and pairs of EEs in the posterior midgut.

(A-A'') A representative image showing single (arrowhead) EEs and pairs (arrow) of EE cells. The ratio of EE cell pairs to single cells is 1:4.5.

The adult fly posterior midguts were stained with anti-Pros (red) and DAPI (blue). Scale bars, 10 μm.

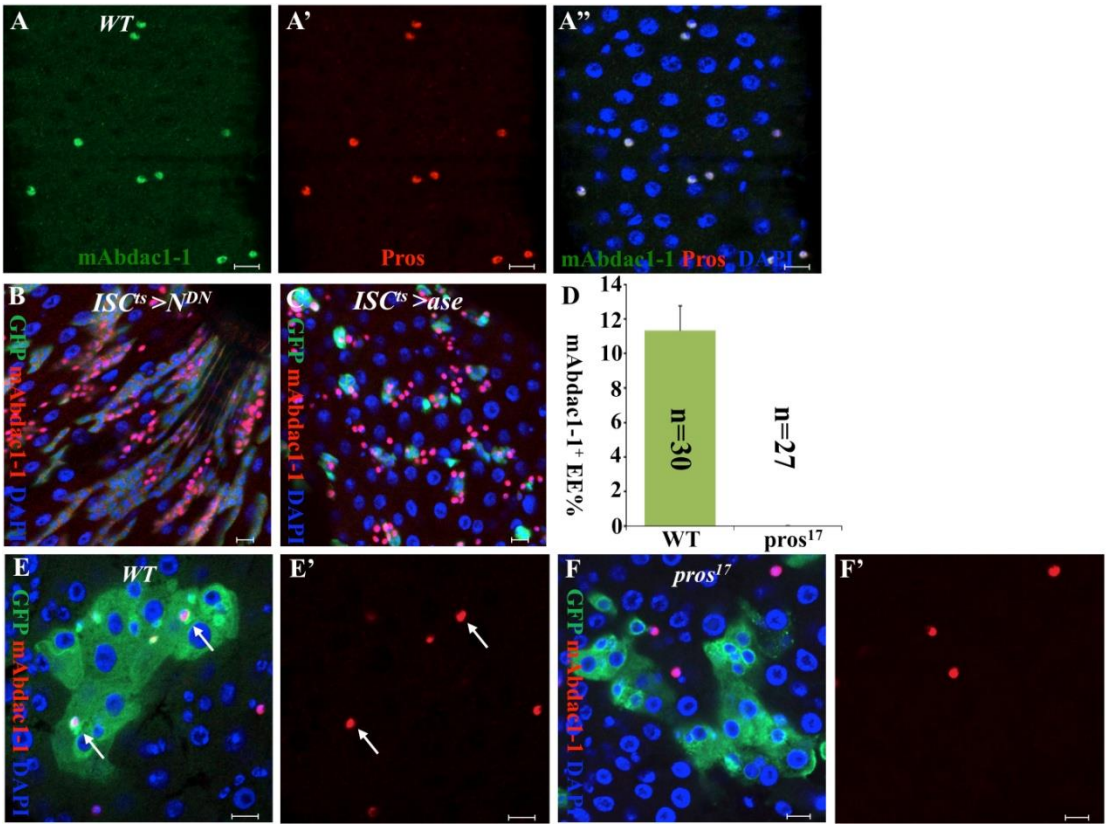

Fig. S6. The identification of transcriptional regulator Dachshund (Dac) as a new EE marker.

(A-A'') The anti-Dac antibody Mabdac1-1 specifically labeled Pros^{+} EEs (Dach, Green; Pros, Red).

(B-C) Excessive EEs caused by the overexpression of UAS-NDN (B) or UAS-Asense (C) were labeled by the anti-Dac antibody.

(D) The quantitative percentages of Dac^{+} EEs in GFP+ clones in E-F'.

(E-F') MARCM clones of wild-type control (E, E') and *pros*^{17} (F, F'). Seven days after clone induction, GFP-marked clones of *pros*^{17} were devoid of Dac^{+} EEs (F, F'), compared to their wild-type counterparts (E, E'). Scale bars, 10 μm.

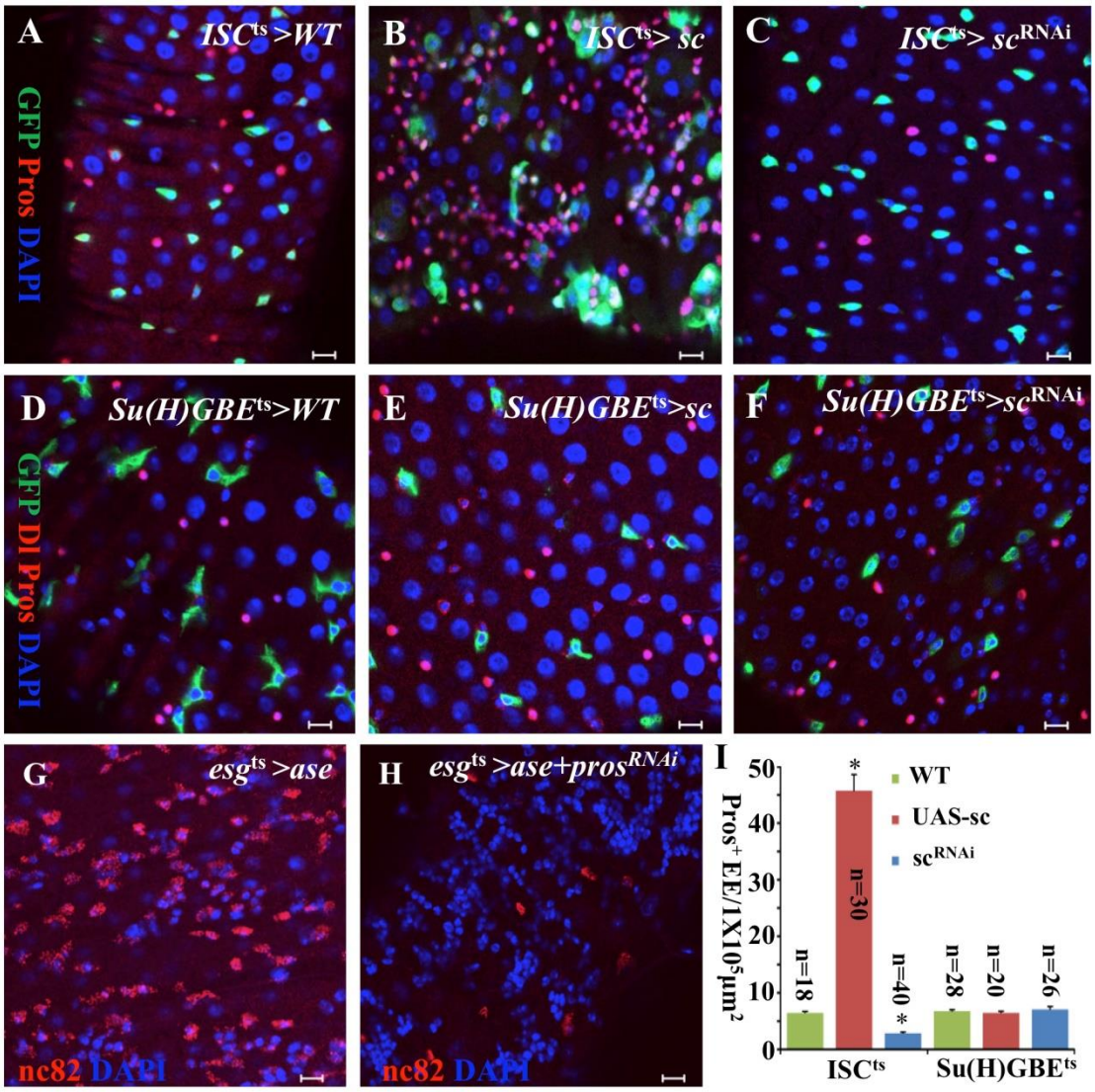

Fig. S7. Sc regulates EE cell fate determination in ISCs.

(A-F) The overexpression (*ISC*^{ts}>*sc*; B) or knockdown (*ISC*^{ts}>*sc*^{RNAi}; C) of *sc* in ISCs, but not in Su(H)GBE^{+} EBs (*Su(H)GBE*^{ts}>*sc*, E; or *Su(H)GBE*^{ts}>*sc*^{RNAi}, F), resulted in significant changes in the percentage of Pros^{+} EE cells, compared to their wild-type counterparts (compare B and C to A; compare E and F to D).

(G) The overexpression of *ase* in ISCs and EBs (*esg*^{ts}>*ase*).

(H) The overexpression of *ase* and *pros*^{RNAi} in ISCs and EBs (*esg*^{ts}>*ase+pros*^{RNAi}). The overexpression of *pros*^{RNAi} suppressed the excess EE phenotype associated with *ase* overexpression, indicating that Pros functions either downstream of or parallel to Ase.

In A-F, the adult fly posterior midguts were stained with anti-GFP (green), anti-Dl (cytoplasmic, red), anti-Pros (nuclear, red), and DAPI (blue). In G-H, the adult fly posterior midguts were stained with nc82 (red) and DAPI (blue). Scale bars, 10 μm.

(I) The quantification of $Pros^{+}$ cells in equal areas in A–F. Data are represented as mean ± s.e.m. $^{*}P<0.01$.

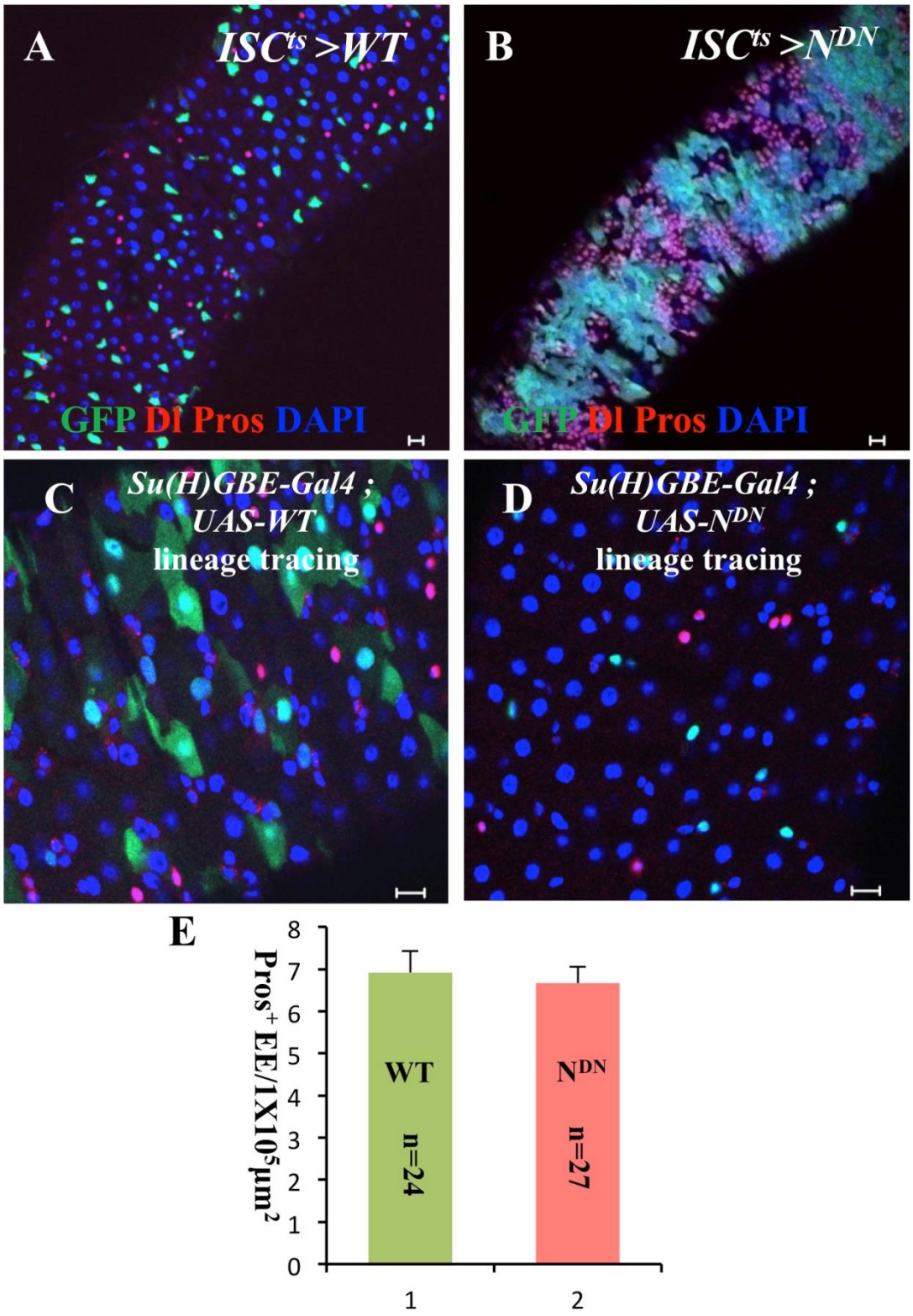

Fig. S8. The function of the N signal in ISCs and Su(H)GBE$^+$ EBs.

(A-B) The expression of N^{DN} in ISCs (ISC^{ts}> N^{DN}; B) resulted in the expansion of both ISC- and EE-like cells, compared to their wild-type counterparts (A).

(C-D) The expression of N^{DN} in Su(H)GBE^{+} EBs using the T-TRACE system (Su-Gal4/T-TRACE> N^{DN}; D) completely blocked differentiation of EBs into ECs, compared to wild-type counterparts (C).

In A-D, the adult fly posterior midguts were stained with anti-GFP (green), anti-Dl (cytoplasmic, red), anti-Pros (nuclear, red), and DAPI (blue). Scale bars, 10 μm.

(E) The quantification of Pros^{+} cells in equal areas in C and D. Data are represented as mean ± s.e.m.